INTERNATIONAL JOURNAL OF HYDROGEN ENERGY 46 (2021) 37545–37555

Available online at www.sciencedirect.com

ScienceDirect

journal homepage: www.elsevier.com/locate/he

# Assessment of geothermal energy use with thermoelectric generator for hydrogen production

M.M. Hadjiat [a,*], A. Mraoui [a], S. Ouali [a], E.H. Kuzgunkaya [b], K. Salhi [a], A. Ait Ouali [a], N. Benaouda [a], K. Imessad [a]

[a] *Centre de Développement des Energies Renouvelables, CDER, 16340, Algiers, Algeria*

[b] *Geothermal Energy Research and Application Center, Izmir Institute of Technology, Urla, İzmir, Turkey*

## HIGHLIGHTS

- Hydrogen production using geothermal energy is cost effective.
- The thermoelectric module is used in converting waste heat to electrical energy.
- TRNSYS software is used to simulate the system.
- 0.5652 kg/m$^2$/year of hydrogen can be produced in Hammam Righa in Algeria using TEG.

## ARTICLE INFO

*Article history:*
Received 31 May 2020
Received in revised form
19 April 2021
Accepted 15 June 2021
Available online 8 July 2021

*Keywords:*
Thermoelectric generator
Geothermal
Seebeck effect
Energy efficiency
Hydrogen production

## ABSTRACT

In this work, a new model for producing hydrogen from a low enthalpy geothermal source was presented. Thermal energy from geothermal sources can be converted into electric power by using thermoelectric modules instead of Organic Rankine Cycle (ORC) machines, especially for low geothermal temperatures. This electrical energy uses the water electrolysis process to produce hydrogen. Simulation and experiments for the thermoelectric module in this system were undertaken to assess the efficiency of these models. TRNSYS software is used to simulate the system in Hammam Righa spa, the temperature of this spring is 70 °C. Obtained results reveal that in hammam righa spa in Algeria, 0.5652 Kg hydrogen per square meter of thermoelectric generator (TEG) can be produced in one year.



## Introduction

Nowadays, global warming and the emission of greenhouse gases caused by the excessive consumption of fossil fuels represent a danger to the planet and the future of humanity. This is due to the increase in energy demand and strong global economic growth. The vast majority of energy production in Algeria originates from fossil fuels (oil and natural gas). Natural gas constitutes 92% of electricity generation and national natural gas consumption is increasing rapidly. Natural gas consumption, which was 15 Mtoe in 2009, reached 24.9 Mtoe in 2018 [1]. The energy transition from fossil fuels to renewable energy sources is becoming more and more crucial to

* *Corresponding author.*
E-mail address: m.hadjiat@cder.dz (M.M. Hadjiat).
https://doi.org/10.1016/j.ijhydene.2021.06.130

**Nomenclature**

| | |
|---|---|
| A | électrolyser electrode surface ($m^2$) |
| F | Faraday constant |
| $I$ | electrical current (A) |
| $I_{el}$ | electrolysis current (A) |
| $I_{sc}$ | short circuit current (A) |
| K | the thermal heat transfer coefficient of the module (W $K^{-1}$) |
| $m_f c_{pf}$ | capacity rate of cooling fluide (W $K^{-1}$) |
| $N_{c,el}$ | number of cells in electrolyzer stack |
| P | electrical power (W) |
| $P_{max}$ | maximum power (W) |
| Q | heat transfer rate (W) |
| $Q_{gen}$ | internal heat generation of the electrolyzer (W) |
| $Q_{loss}$ | electrolyzer heat lost to the ambient (W) |
| $r$ | electrolyzer empirical parameter |
| R | electrical resistance of the module (Ω) |
| $R_L$ | load resistance (Ω) |
| $R_{t,el}$ | thermal resistance of electrolyzer (W $K^{-1}$) |
| s | electrolyzer empirical parameter |
| t | electrolyzer empirical parameter |
| T | temperature (K) |
| $T_{ambient}$ | ambient temperature (K) |
| $T_E$ | electric heater temperature (K) |
| UA | thermal conductance of heat exchanger (W $K^{-1}$) |
| $U_{el}$ | electrolyzer voltage (V) |
| $U_{rev}$ | electrolysis reversible voltage (V) |
| $U_{tn}$ | electrolyzer thermoneutral voltage (V) |
| V | voltage (V) |
| $V_{oc}$ | open circuit voltage (V) |

*Greek symbols*

| | |
|---|---|
| $\alpha$ | Seebeck coefficient (V $K^{-1}$) |
| $\Delta T$ | temperature difference (K) |
| $\varepsilon$ | heat exchanger effectiveness |
| $\eta_F$ | Faraday efficiency |

*Subscripts*

| | |
|---|---|
| c | cold side |
| h | hot side |

*Abbreviations*

| | |
|---|---|
| ORC | Organic Rankine Cycle |
| TEG | thermoelectric generator |
| TE | thermoelectric |

avoid an energetic crises and global warming in the future. The current energy policy of Algeria gives the priority to renewable energy.

Hydrogen represents a promising energetic vector if it is produced by renewable energy. Hydrogen energy is considered to be the energy of the future, as it is a clean energy and is storable compared to other renewable energy sources. Some researchers worked on the extraction of hydrogen from hydrogen sulfide ($H_2S$). Investigating both chemical and thermal methods for hydrogen removal from hydrogen sulfide, Ouali et al. [2] has proposed to produce hydrogen from hydrogen sulfide in a geothermal area in Algeria. This process is an opportunity to produce hydrogen with less energy and to minimize the presence of $H_2S$ in the environment to an extremely low level. Petrov et al. [3] has proposed to extract hydrogen from hydrogen sulfide contained in the water of the Black sea by electrochemical process, the economic and the environmental aspects of the process was investigated.

Karapekmez et al. [4] have presented a new model for hydrogen production using AMIS technology (for abatement of mercury and hydrogen sulfide) for hydrogen production from $H_2S$. The hydrogen sulfide has trapped inside the AMIS unit and sent to an electrolyzer system in order to decompose it into hydrogen and sulfur dimer. The calculated energy and exergy efficiencies of the process are 27.8% and 57.1% respectively when the inlet temperature of $H_2S$ is 150 °C. In another study, Karapekmez et al. [5] have suggested a novel model for hydrogen production from hydrogen sulfide using solar and geothermal based combined energy systems. The system consists of solar parabolic trough collectors and geothermal energy source to generate six outputs which is power, cooling, heating, drying air, domestic hot water and hydrogen. The results show that the overall energy and exergy efficiencies of the system are 78.37% and 58.40% in the storing period, respectively.

Although the production of hydrogen from hydrogen sulfide was beneficial for the environment and cost effective, this method did not have great success. The production of hydrogen by the electrolysis of water is the most widely used method in the world. Boudries et al. [6] have recommended a model to produce hydrogen using solar PV as an energy source. Mraoui et al. [7] have examined experimental and simulation of the production of hydrogen by a proton exchange membrane (PEM) electrolyzer using solar photovoltaic PV as an energy source. Baykara [8] has shown that electrolysis of water at high temperatures is thermodynamically more efficient than at low temperatures. However, the inconvenience in these systems is that the production of hydrogen depends on the intensity of solar radiation.

In fact, the production of hydrogen by electrolysis of water using geothermal energy is a non-polluting and environmentally friendly process and also this method has many advantages. Indeed, geothermal energy is constantly and durably provided in the form of heat. Commonly, this energy is converted by Organic Rankine Cycle (ORC) machine into electricity and then hydrogen. The hydrogen can be easily stored and transported, and this is the advantage of this process. The production of hydrogen by geothermal energy has been widely discussed among researchers in the world.

Balta et al. [9] have analyzed the high-temperature electrolysis process where geothermal water is used as the heat source. The same group [10] investigated various options for geothermal-based hydrogen production systems and their technical, operational and efficiency aspects.

Kanoglu et al. [11] have developed and analyzed three models for hydrogen liquefaction by geothermal energy. In a recent study, Kanoglu et al. [12] have also investigated the use of geothermal production for hydrogen production and liquefaction. Four models were considered and analyzed thermodynamically including the use of geothermal work output; the work input for an electrolysis process (case 1), the use of a part of geothermal heat to produce work for the electrolysis process and the other part for preheating water (case 2), the use of geothermal heat to preheat the water in a high temperature electrolysis process (case 3) and the use part of geothermal work for electrolysis and the remaining part for liquefaction (case 4). The results show that the produced hydrogen amount by one kg of geothermal water at 200 °C is higher in case 3 compared to other cases.

Yilmaz et al. [13–15] have considered seven models for hydrogen production and liquefaction by geothermal energy and were performed their thermodynamic and simple economic analyses. It is estimated that the cost of hydrogen production and liquefaction ranges between 0.979 \$/kg $H_2$ and 2.615 \$/kg $H_2$ depending on the model. The results show that the cost of hydrogen production and liquefaction decreases as the geothermal water temperature increases. Therefore, this system is more efficient in geothermal sources with high-enthalpy.

In Algeria, geothermal energy can be considered as a low enthalpy energy source and the temperature of the hottest spring is situated in the range of 30–70 °C [16]. Therefore, all systems based on ORC machines cannot be considered as cost effective. Nevertheless, Holdmann [17] has reported ORC in Chena Hot Spring, Alaska, geothermal heat sources with temperatures 73 °C, can produce a capacity of 210 kW and an efficiency of 8.2%, however, water cooling fluid temperature is 4.4 °C during all the year. Hadi Ganjehsarabi [18] has proposed to use for low temperature heat source, a mixture of butane, pentane and iso-pentane as working fluid in Organic Rankine Cycle (ORC) integrated with proton exchange membrane (PEM) electrolyzer, however, the lowest temperature of heat source must be 70 °C.

Recently, the use of thermoelectric technology in waste heat recovery have been developed in many research laboratories. The application of this technology to produce renewable energy has become very useful. Chávez-Urbiola et al. [19] have used concentrated solar energy to heat one side of a thermoelectric module to produce renewable electricity. An efficiency of 4% was obtained with such a system under the considered operating conditions. Zare and Palideh [20] have integrated thermoelectric modules into a Kalina cycle to improve its efficiency. The cycle is driven by geothermal energy to produce renewable electricity. The authors have reported a 7.3% increase in energy and energy efficiency by integrating thermoelectric generators (TEGs). The economic evaluation revealed that the proposed system would be profitable if the added TEG costs lower than 6.4 \$/W. Khanmohammadi et al. [21] have proposed an improvement of a geothermal system producing electricity and hydrogen by electrolysis by recovering waste heat from condensers using thermoelectric modules. Based on the economic study performed, the authors find that if the cost of the TEGs is less than 6 \$/W, the payback period is quite reasonable. Ziapour et al. [22] have used a thermoelectric generator to replace an Organic Rankin Cycle. The system is a solar pond power plant. The authors have also investigated the possibility of coupling the two technologies in order to evaluate the performance. The results show that efficiencies are increased by 0.2% compared to an ORC alone, giving an overall efficiency of 2.6%. Habibollahzade et al. [23] have studied a system using thermopiles combined with an Organic Rankin Cycle. The thermopiles are connected to a PEM electrolyzer to produce renewable hydrogen. However, the temperature of the geothermal source is 200 °C. Hydrogen production under optimal conditions is 300 kg/day.

In renewable energy systems, the use of thermoelectric modules is generally used to recover heat that would otherwise be lost [24]. Thermoelectric modules are usually combined with an Organic Rankin Cycle to improve their efficiency. However, these systems require a temperature of the geothermal source of around 160–200 °C. In Algeria, the temperatures of geothermal sources have generally low temperatures. The majority of geothermal sources have an average temperature of 70–90 °C.

The aim of this work is to find a new model for hydrogen production adapted to Algerian's hot spring. The use of thermoelectric modules instead of an ORC machines is recommended in this case. In this study, we propose a new method for the production of hydrogen by geothermal energy using low enthalpy. The system uses a thermoelectric generator to produce the electricity required for the electrolysis of water. The hydrogen is produced by an alkaline electrolyzer at the temperature of the geothermal source. A TEC1-12706 thermoelectric module generates electricity, but it is necessary to maximize the power produced. Experiments will be carried out to determine the maximum power according to the temperature of the hot and cold sides of the module. Thereafter, simulations using the TRNSYS software will be used to calculate the amount of hydrogen that can be produced at the Hammam Righa site where the temperature of the geothermal source is 70 °C.

## System description

Fig. 1 shows a hydrogen production system and this model is mainly composed of a thermoelectric module system and an alkaline electrolyzer. The role of thermoelectric modules is to generate electricity by creating a temperature difference between the hot side and the cold side. To get this temperature difference, we will use water from a hot spring as a renewable energy source and a cooling system that uses ambient air as a cooling fluid.

For a better analysis of the system shown in Fig. 1, we divided the study into two parts. In the first part, there are studies on the thermoelectric generator used to generate the electrical energy required for the electrolysis of water. A thermoelectric module has been experimentally characterized to determine the maximum power using geothermal energy as a renewable energy source. In the second part, the amount of the hydrogen produced according to the electrical energy produced by TEG was determined. TRNSYS software was used to simulate hydrogen production in the thermal spa.

The basic principle of thermoelectric materials is the Seebeck effect, which was discovered by Thomas Seebeck. As shown in Fig. 2, a typical thermoelectric element consists of pairs of p and n type semiconductors interconnected by a metallic conductor such as copper. The thermoelectric element TE is electrically connected in series and thermally in parallel and is sandwiched between two ceramic plates to form a thermoelectric module. When a temperature difference $\Delta T$ (K) between the TEG surfaces is created, the TEG produces electrical voltage. The voltage value is directly

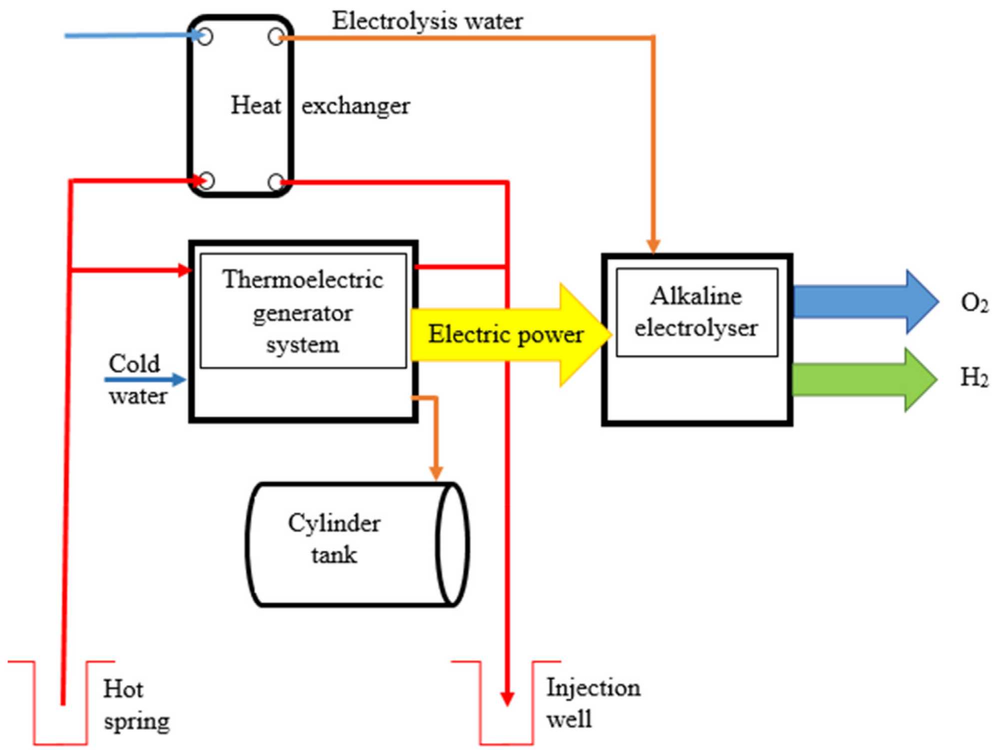


**Fig. 1 – Schematic of Thermoelectric generator mounted with alkaline Electrolyzer.**

proportional to the temperature difference as shown in equation (1) [25].

$$V = \alpha.\Delta T \tag{1}$$

where $\alpha$ (V/K) is the Seebeck coefficient of the thermoelectric generator and $\Delta T$ (K) is the temperature difference between the two surfaces of the module.

## Thermoelectric generator (TEG)

### *Analytical model of TEG*

The thermoelectric device can be used as a thermoelectric generator or thermoelectric cooler. TEG converts thermal energy from a temperature difference to electrical energy by the Seebeck effect, whereas TE cooler converts electrical energy into a temperature difference by the Peltier effect.

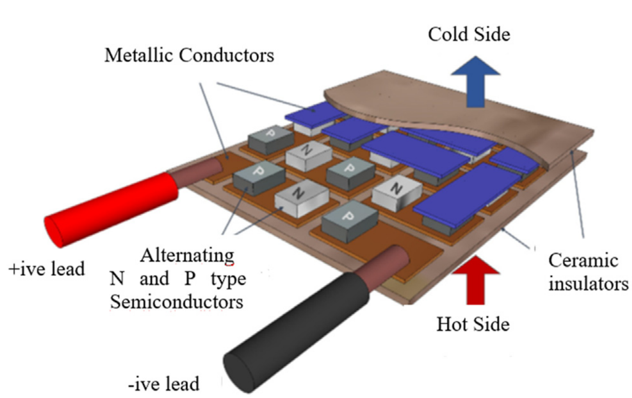


**Fig. 2 – Structure of thermoelectric module.**

Fig. 3 shows the equivalent electrical diagram of a thermoelectric generator. The thermoelectric module which is connected to a load is subjected to a temperature difference between its two surfaces, it functions as a generator. The inlet and outlet heat in TE module used as a generator is expressed by the following equations [26].

$$Q_c = \alpha I T_c + 0.5 I^2 R + K \Delta T \tag{2}$$

$$Q_h = \alpha I T_h - 0.5 I^2 R + K \Delta T \tag{3}$$

Here, $Q_h$ (W) represent the thermal energy absorbed by the hot surface and $Q_c$ (W) represent the ejected thermal energy from the cold surface. $T_h$ (K) is the temperature of the hot side and $T_c$ (K) is the temperature of the cold side. $\alpha$ (V/K) is the Seebeck coefficient, R (Ω) is the total resistance of the module, $I$ (A) is the current drawn from the TE module and $K$ (W/K) is the thermal heat transfer coefficient of the module.

The output power of the TE module is $P = Q_h - Q_c$, P is obtained from equations (2) and (3) and is expressed as the following equation (4)

$$P = \alpha \Delta T - I^2 R \tag{4}$$

When a load is connected to the TE module, the current $I$ (A) and the voltage $V$ (V) at the load are given as in equations (5) and (6) below:

$$I = \alpha \Delta T / (R + R_L) \tag{5}$$

$$V = \alpha \Delta T R_L / (R + R_L) \tag{6}$$

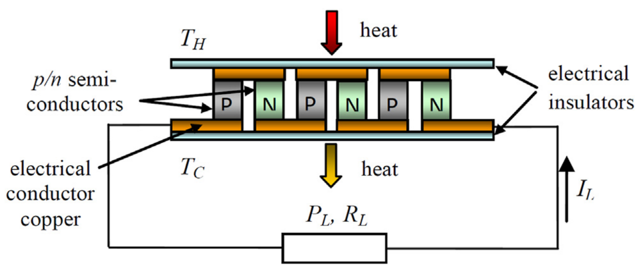


**Fig. 3 – Thermoelectric module in TEG mode.**

The power $P = I.V$, is deduced from the relation of equations (5) and (6):

$$P = \alpha^2 \Delta T^2 R_L / (R + R_L)^2 \quad (7)$$

The Seebeck coefficient and internal resistance of a TEG are determined by measuring experimentally the open-circuit voltage ($V_{oc}$), the short circuit ($I_{sc}$), and the temperature difference between hot and cold sides of the TEG. The Seebeck coefficient is calculated using equation (8).

$$\alpha = V_{oc}/\Delta T \quad (8)$$

The internal resistance of the TEG is the rate of the open-circuit voltage ($V_{oc}$) to the short circuit current ($I_{sc}$) and is given as equation (9).

$$R = V_{oc}/I_{sc} \quad (9)$$

The maximum power ($P_{max}$) is obtained when $R = R_L$. By using equations (8) and (9), $P_{max}$ can be evaluated theoretically as equation (10).

$$P_{max} = \alpha^2 \Delta T^2 / 4R \quad (10)$$

### *Characterization of individual TEG*

In order to assess the hydrogen production of our system, the commercially available $Bi_2Te_3$ TE module (TEC1-12706) was used. The TEC1-12706 is a 40 × 40 mm Thermoelectric Peltier Module, with the simple application of the Peltier Thermoelectric Effect. The module include 127 semiconductor couples in the area of 40 × 40 mm which very effectively cools and heats up to 90 °C. The maximum operating temperature is 138 °C. The life expectancy of the module is about 200,000 h. The module is mainly used to warm or cool surfaces, but it can take advantage of a temperature differential to generate electricity. The datasheet does not contain details about the electrical current that can be generated using this module. Thus, experiments are necessary to determine the IV curves according to the differential temperature applied on each side of the module.

Although they have the disadvantage of a rather low power density, the TEC1-12706 module generates 0.25 W for a surface of 16 $cm^2$ when it is subjected to a temperature difference of 50 °C. Also, thermoelectric modules can deteriorate if they are subjected to a high temperature. It is necessary to take certain precautions during their installation so that they offer the best performance [27].

As shown in Fig. 4, the experimental device consists of the following components according to this order: electrical heater, aluminum plate with thermocouple $T_h$, TEC1-12706 thermoelectric module, aluminum plate with thermocouple $T_c$ and finally heat sink with fan cooler. Thermocouples allow to measure the temperature difference $\Delta T = T_h - T_c$.

The electric heater is used to heat the hot side of the module; the heat flow through the hot side heat exchanger $Q_h$ can be modeled as

$$Q_h = UA_h(T_E - T_h) \quad (11)$$

Where $T_E$ is the temperature of the electric heater, $UA_h$ is the overall thermal conductance of the hot side heat exchanger from the electric heater to the hot side of the TEC module. The heat sink is used to cool the cold side of the module. The method of the effectiveness number of transfer units (NTU) is used for the cold side heat exchanger [28], the heat transfer rate $Q_c$ can be expressed as

$$Q_c = \varepsilon_c m_f c_{pf} (T_c - T_{ambient}) \quad (12)$$

Where $T_{ambient}$ and $m_f c_{pf}$ are respectively the ambient temperature and the heat capacity rate of the cooling fluid, $\varepsilon_c$ is the heat exchanger effectiveness and can be written as

$$\varepsilon_c = 1 - exp(UA_c / m_f c_{pf}) \quad (13)$$

Where $UA_c$ is the overall thermal conductance of the cold side heat exchanger from the cold side of the TEC module to the cooling fluid. Temperature measurements were made with K type thermocouple sensors. The current and tension were recorded by using a multimeter EXTECH EX542 data logger. Whereas the temperature were recorded with an EXTECH SDL200 data logger.

The thermoelectric module connects to a variable resistance load. A temperature difference between the two sides of the module is applied and by varying the resistance of the load, the value of the voltage and current supplied by the module is determined experimentally. Repeating the operation with varying the temperature of the electric heater, the variation of the maximum power is obtained versus temperature difference.

The properties of this module TEC1-12706 such as open-circuit voltage ($V_{oc}$) and short circuit current ($I_{sc}$) depend on the difference of the temperature $\Delta T$, these properties provided by experimental measurements are given in polynomial form as follows:

$$V_{oc} = 0.2717 + 0.0135.\Delta T + 7.7240.10^{-4}.\Delta T^2 - 6.3907.10^{-6}.\Delta T^3 \quad (14)$$

$$I_{sc} = 0.1113 + 6.1301.10^{-4}.\Delta T + 2.1258.10^{-4}.\Delta T^2 - 1.8275.10^{-6}.\Delta T^3 \quad (15)$$

### *Results*

The experimental results are presented in Figs. 5–7. Figs. 5 and 6 show the curve of output voltage and power versus current respectively. Fig. 7 shows the maximum power versus temperature difference (ΔT). The experimental and theoretical results are in harmony with each other. Fig. 7 is shown that power increases with the temperature difference.

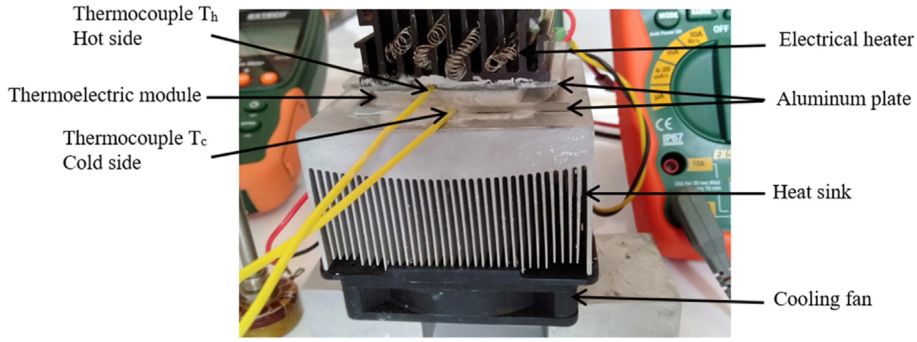


**Fig. 4 – Experimental components and set up.**

## Electrolyzer operation

The alkaline water electrolyzer has a long history of use in the chemical industry (see Fig. 8). This type of electrolyzer is characterized by having two electrodes operating in a liquid alkaline electrolyte solution of potassium hydroxide (KOH). These electrodes are separated by a diaphragm, separating the product gases and transporting the hydroxide ions (OH-) from one electrode to the other. The diaphragm further avoids the mixing of the produced hydrogen and oxygen at the cathode and anode respectively. Typically, Nickel-based metals are used as the electrodes for alkaline water electrolysis. The advantages of alkaline water electrolysis are mainly: Cheaper catalysts concerning the platinum metal group based catalysts used for PEM water electrolysis. Higher durability due to an exchangeable electrolyte and lower dissolution of anodic catalyst. Higher gas purity due to lower gas diffusivity in alkaline electrolyte.

Generally, the operating temperature of the electrolyzer is between 50 °C and 70 °C, allowing it to maximize its overall efficiency.

Ideally, for a single electrolysis cell, the voltage required to decompose water is 1.23 V. This is the reversible voltage obtained by the Nernst equation. However, in reality, there are losses due to various resistance in the cell. The losses can be classified as activation losses, which quantify for slow electro-

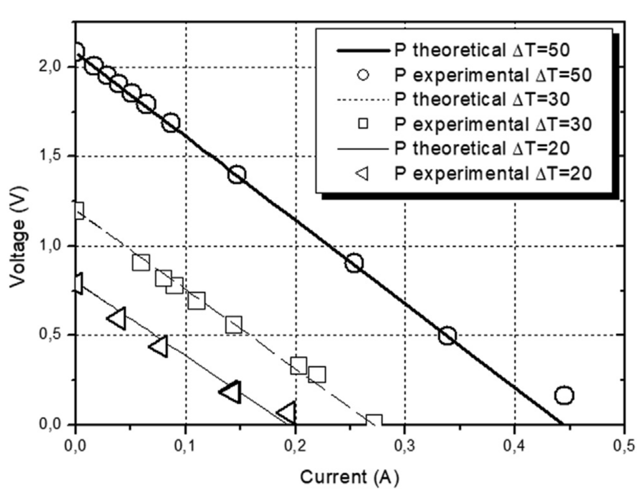


**Fig. 5 – Output voltage-current for different ΔT.**

kinetics, ohmic losses in the cell and concentration losses, which occur at higher current density due to improper mass transfer of the species.

The electrolyzer cell potential can be evaluated from equation (16):

$$U_{el} = U_{rev} + r/AI_{el} + s\log(t/AI_{el} + 1) \quad (16)$$

$U_{rev} = \Delta G/nF = 1.23V$. The empirical parameters r, s, and t are obtained by curve-fitting manufacturers' data.

$$r = r_1 + r_2 T \quad (17)$$

$$t = t_1 + t_2/T + t_3/T^2 \quad (18)$$

The amount of hydrogen produced is given by

$$\eta_{H_2} = \eta_F N_{c,el} I_{el}/(nF) \quad (19)$$

where $\eta_F$ is the Faraday efficiency which is the ratio of actual hydrogen produced to theoretical maximum possible production. $N_{c,el}$ is the number of cells in the electrolyzer stack.

The performance of the electrolyzer is dependent on the operating temperature. When the temperature increases the efficiency increases. The temperature can either be assumed constant or can be calculated by using a thermal model. A lumped thermal capacitance model is used to predict the temperature of the electrolyzer [29]:

$$C_t dT/dt = Q_{gen} - Q_{loss} - Q_{cool} \quad (20)$$

$Q_{gen}$ is the internal heat generation of the electrolyzer, $Q_{loss}$ is the heat lost to the ambient, and $Q_{cool}$ is the amount of cooling required to keep the electrolyzer at a rated condition (maximum temperature 80 °C). These are given as follows:

$$Q_{gen} = N_{c,el}(U_{el} - U_{tn})I_{el} \quad (21)$$

where

$$U_{tn} = \frac{\Delta H}{nF} = 1.48V \quad (22)$$

$$Q_{loss} = 1/R_{t,el}(T - T_{ambient}) \quad (23)$$

$R_{t,el}$ the overall thermal resistance of electrolyzer (W/K).

Generally, the temperature of the electrolyzer is limited for safety reasons to 80 °C. If the temperature is below 80 °C there is no cooling ( $Q_{cool} = 0$), if the temperature is above, $Q_{cool}$ is calculated to maintain the temperature below 80 °C. The

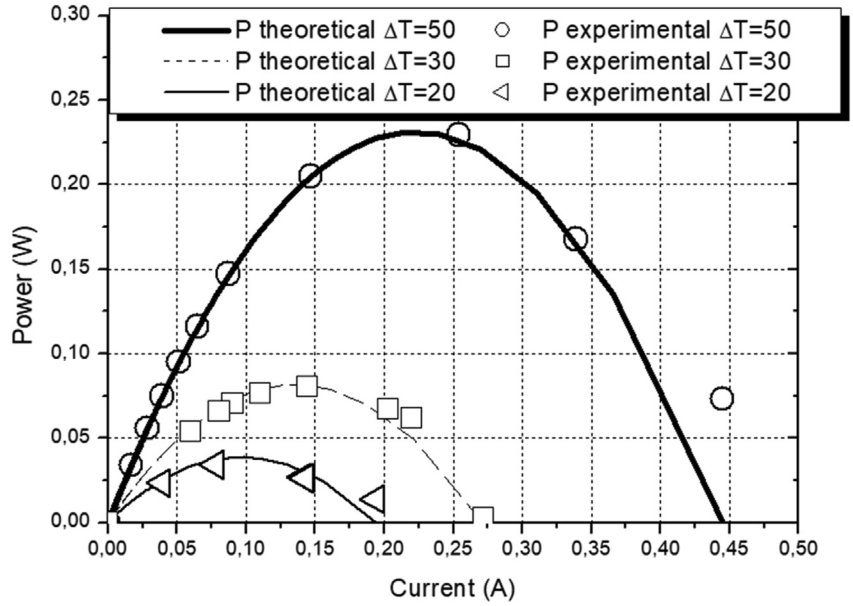


**Fig. 6 – Power for different ΔT.**

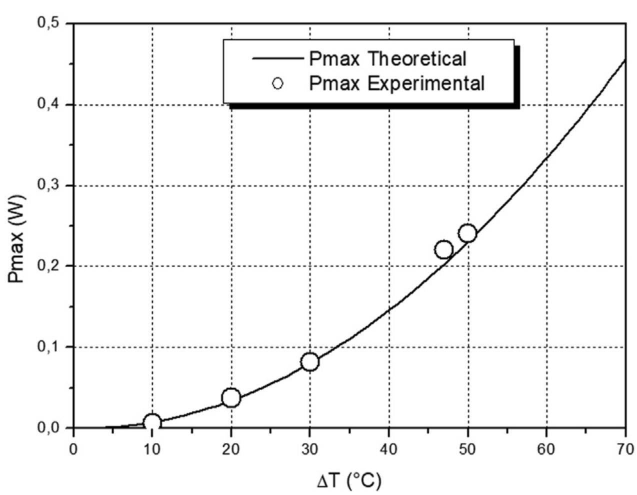


**Fig. 7 – Maximum power as a function of ΔT.**

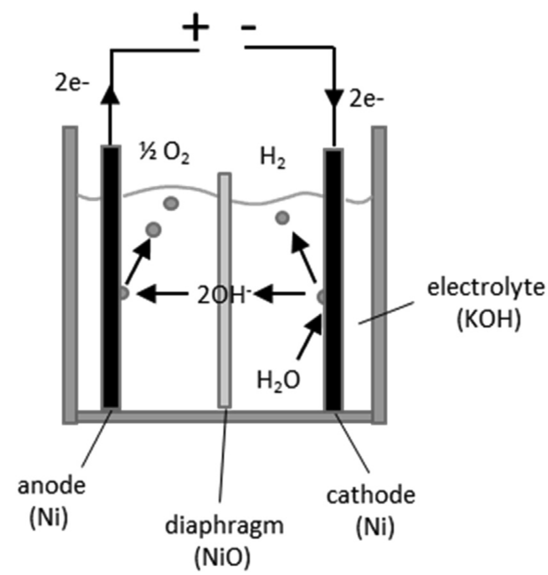


**Fig. 8 – Typical alkaline electrolyzer.**

electrolyzer used in this study is a 21 cells stack electrolyzer (48 V) and is assumed to be working under a pressure of 7 bars. The energy used by the electrolyzer system (parasitic load) is assumed to be 0.6 W/kW during the shutdown, and 3 W/kW during operations (hydrogen production) [29].

## System simulation

In a geothermal spring, the water comes out at a temperature between 70 °C and 90 °C.The water to be used is usually cooled in heat exchangers, thus this thermal energy is commonly lost. It is proposed to recover this energy by generating electricity in order to generate renewable hydrogen. The thermoelectric module produces electricity by being exposed to a temperature gradient. This electricity is used to power a high-power alkaline electrolyzer. The thermal energy is thus recovered by producing hydrogen that can be stored for later use.

The geothermal source of Hammam Righa was chosen to calculate the potential for hydrogen production using this system. The thermal station is in the wilaya of Aïn Defla, 90 km south-east of the city of Algiers (capital of Algeria). The temperature of the thermal spring reaches 70 °C most of the year.

To simulate the production of hydrogen, an electrolyzer with known characteristics was chosen and adapted to the system described in Ref. [30]. The system has been modified to use the thermoelectric modules as a source of electricity. Hydrogen production was thus evaluated for the whole year using meteorological data from Hammam Righa [31].

## Result and discussion

Experimental tests on TEC1-12706 thermoelectric modules show that the mathematical models describing characteristic IV are applicable. It was noted that the I–V curve of the TEG is linearly decreasing (Fig. 5). As the voltage increases, the current decreases, the mean absolute percentage error between the experimental IV points and the regression curves is in the range of 0.3–2.5%. Same experiments were conducted by Hsu et al. [32]. The authors obtained similar curves on TMH400302055 TEG module (Wise Life Technology, Taiwan).

The linear curve in Fig. 6 gives a quadratic relationship for power versus current. The P–I curve has an extremum that represents the maximum power that can be delivered by the TEG module under the given operating conditions. Different techniques can be applied to extract this maximum power. The most popular of the maximum power point tracking (MPPT) techniques is perturb and observe. The power efficiency of a dc/dc system with MPPT is typically 80–85% [33,34].

As the temperature difference between the hot and cold sides of the TEG increases, the power output increases. The relationship between power and temperature difference is quadratic. Power becomes much greater when the temperature gradient is high (Fig. 7). The same trend was observed by Refs. [32,35,36].

By characterizing a thermoelectric module Liu et al. [35,36] was able to build a 500 W and 1 kW generator. The generator uses a low-temperature geothermal source to produce renewable electricity. The 500 W power generator used 96 thermoelectric modules and it provided its full power at a temperature difference of 200 °C. The 1 kW generator used 600 modules and it delivered its full power at a temperature difference of 120 °C. The flow of hot and cold fluid is counter-current. The designed system has demonstrated the feasibility of using low temperature geothermal energy to produce renewable electricity. With a capacity factor of 90% the cost of these systems can be lower than a standard PV or Wind systems.

The studied system consists of a thermoelectric generator, a dc/dc converter with MPPT function and an alkaline electrolyzer to produce renewable hydrogen. The thermoelectric generator was subjected to a temperature gradient: on one side the geothermal source and on the other side the ambient air. The power delivered by the thermoelectric generator depends on the temperature of the hot source and the cooling temperature.

The studied system was simulated using TRNSYS software. Fig. 10 shows the schematic used in the simulations. The thermoelectrical module has no model in TRNSYS. It was integrated by using a set of equations that calculate the power supplied as a function of the geothermal water temperature and the ambient air temperature. A power converter was included between the generator and the electrolyzer. The latter allows the control of the electrolyzer under specific operating conditions. The electrolyzer is of alkaline type, its power has been set at 1 kW. The power of the thermoelectric generator has been set at 1.2 kW.

Simulation results for one year of system operation are shown in Fig. 9. Simulation results were reported by a square meter of thermoelectric module surface. This operation allows to compare this technology with the production of hydrogen using photovoltaic modules. Thus, the potential of hydrogen production can be evaluated, and to calculate the required hydrogen requirement, it will be sufficient to multiply by the surface area.

The monthly productions were shown in Table 1. Due to the temperature gradient, the warmest month (June) has the lowest production and the coldest month (January) has the highest production. The temperature of the geothermal source hardly varies. It is the cooling temperature of the thermoelectric generators that determines the power produced.

Hammam Righa is a thermal spa and is used for medical or touristic reasons to carry out thermal cures (external hydrotherapy). The geothermal water has unique properties allowing a person to get back into shape and get back to health. Hammam Righa has an average temperature of 70 °C, making large-scale energy exploitation inefficient. In air exchangers for use in baths, the temperature of the source is lowered and this causes the heat to be wasted. The use of thermoelectric modules that recover the geothermal heat would allow the recovery of this energy that would be lost without this process. Simulation results were showed that it was possible to produce 0.5652 kg Hydrogen per square meter of TEG in one year.

The potential for hydrogen production from geothermal sources is much less than from solar photovoltaic energy. The hydrogen production in the Hammam Righa region is about 3.2 $kgH_2/m^2$/year using a standard sized photovoltaic generator [24]. This production is about 6 times the geothermal production. In order to reach the same level, it is necessary to obtain better efficiency from thermopile modules. Therefore, this process would represent a gain if the hydrogen produced from geothermal energy would be lost without this process.

The energy efficiency of the system has not been evaluated. The purpose of this study is to analyze hydrogen production. The study can be completed by an economic evaluation, however, studies have shown that a TEG cost of less than 6 $/W makes this type of installation profitable [21]. An evaluation of other geothermal sources could give an overall idea of the potential of this technique in Algeria.

The electricity generated by the thermoelectric generators is of the direct current type. The direct current electricity obtained can be used to feed various facilities or houses by using inverters that convert to alternating current. It is possible to inject this electricity into the electrical grid. In our study, this renewable energy is used to produce renewable hydrogen. Studies on converting low enthalpy geothermal energy to hydrogen have received little attention. The use of geothermal energy at low temperatures is not much studied because of the low efficiency of a conventional conversion system. Because the higher the temperature increases, the higher the conversion efficiency ($1-T_{Cold}/T_{Hot}$). If the temperature is low, the efficiency is quite low.

Viewed from a broad perspective, conversion to Hydrogen allows to expand the range of use of geothermal resources and at the same time allows us to obtain high yields from the source. Various systems using renewable energies (particularly photovoltaic energy) to produce hydrogen have been studied and tested. The feasibility of such systems has been extensively demonstrated through the studies by Gibson and Kelley [37,38].

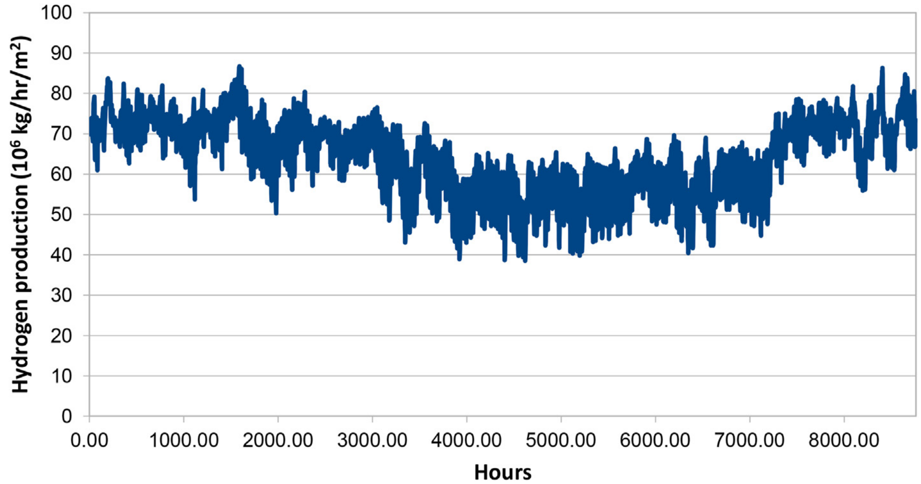


**Fig. 9 – Hydrogen production at Hammam Righa site.**

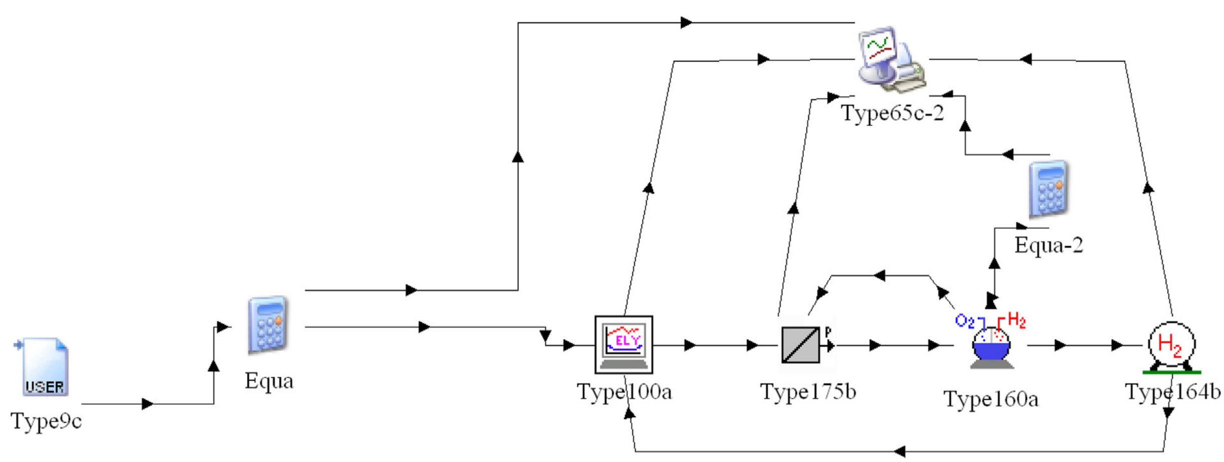


**Fig. 10 – Simulated system.**

**Table 1 – Monthly hydrogen production.**

| Month | Production |
|---|---|
| January | 0.0547 Kg $H_2/m^2$/month |
| February | 0.0481 Kg $H_2/m^2$/month |
| March | 0.0525 Kg $H_2/m^2$/month |
| April | 0.0496 Kg $H_2/m^2$/month |
| May | 0.0473 Kg $H_2/m^2$/month |
| June | 0.0403 Kg $H_2/m^2$/month |
| July | 0.0405 Kg $H_2/m^2$/month |
| August | 0.0411 Kg $H_2/m^2$/month |
| September | 0.0416 Kg $H_2/m^2$/month |
| October | 0.0439 Kg $H_2/m^2$/month |
| November | 0.0516 Kg $H_2/m^2$/month |
| December | 0.0538 Kg $H_2/m^2$/month |

## Conclusion

In this study, studies and investigations on the efficiency of hydrogen production from geothermal energy using thermoelectric modules were made. Experiments were carried out to model the thermoelectric module TEC1-12706. The current-voltage curves were drawn, which allowed modeling the power of electricity produced according to the difference between hot and cold temperature. The model used was very close to the experiments with a maximum deviation of 2.5%.

- From the experimental data, a more complex hydrogen production system was simulated. The system was powered by a geothermal source to provide the heat required for the production of renewable electricity. This electricity was used by an electrolyzer to produce renewable hydrogen.
- The performance of the TEGs is more interesting at high temperature gradients. However, the characteristics of the geothermal sources in Algeria is their low enthalpy. The temperature of the sources varies between 70 °C and 90 °C. A use for purely energy purposes cannot be efficient in these cases. The heat used by the TEGs was the heat that is just necessary to cool the water for use in thermal baths.
- Hydrogen production at the hammam Righa site was evaluated in this study. It was found that it is possible to produce 0.56 kg of hydrogen per square of TEG in one year.

The production of hydrogen depends on the temperature difference between the geothermal source and the ambient air. The greater the temperature difference, the greater the production of hydrogen.

- The conversion using the TEC1-12706 module was investigated in this study. If the thermoelectric module has better efficiency, electricity production would be more important. The future development of this technology could in the long-term lead to more interesting efficiency, which would contribute to the emergence of this technique for power generation.

Although the hydrogen potential produced by this system is lower than that produced by a system using photovoltaic energy, the advantage of this technique is that it uses energy that would be completely lost.

## Declaration of competing interest

The authors declare that they have no known competing financial interests or personal relationships that could have appeared to influence the work reported in this paper.

REFERENCES

[1] Bouraiou A, Necaibia A, Boutasseta N, Mekhilef S, Dabou R, Ziane A, Sahouane N, Attoui I, Mostefaoui M, Touaba O. Status of renewable energy potential and utilization in Algeria. J Clean Prod 2020;246:119011.
[2] Ouali S, Chader S, Belhamel M, Benziada M. The exploitation of hydrogen sulfide for hydrogen production in geothermal areas. Int J Hydrogen Energy 2011;36:4103–9.
[3] Petrov K, Baykara SZ, Ebrasu D, Gulin M, Veziroglu A. An assessment of electrolytic hydrogen production from H2S in Black Sea waters. Int J Hydrogen Energy 2011;36:8936–42.
[4] Karapekmez A, Dincer I. Modelling of hydrogen production from hydrogen sulfide in geothermal power plants. Int J Hydrogen Energy 2018;43(23):10569–79.
[5] Karapekmez A, Dincer I. Thermodynamic analysis of a novel solar and geothermal based combined energy system for hydrogen production. Int J Hydrogen Energy 2020;45:5608–28.
[6] Boudries R, Khellaf A, Aliane A, Ihaddaden L, Khida F. PV system design for powering an industrial unit for hydrogen production. Int J Hydrogen Energy 2014;39:15188–95.
[7] Mraoui A, Benyoucef B, Hassaine L. Experiment and simulation of electrolytic hydrogen production: case study of photovoltaic-electrolyzer direct connection. Int J Hydrogen Energy 2018;43:3441–50. https://doi.org/10.1016/j.ijhydene.2017.11.035.
[8] Baykara SZ. Hydrogen production by direct solar thermal decomposition of water, possibilities for improvement of process efficiency. Int J Hydrogen Energy 2004;29:1451–8.
[9] Balta MT, Dincer I, Hepbasli A. Thermodynamic assessment of geothermal energy use in hydrogen production. Int J Hydrogen Energy 2009;34:2925–39.
[10] Balta MT, Dincer I, Hepbasli A. Potential methods for geothermal-based hydrogen production. Int J Hydrogen Energy 2010;35:4949–61.
[11] Kanoglu M, Dincer I, Rosen MA. Geothermal energy use in hydrogen liquefaction. Int J Hydrogen Energy 2007;32(17):4250–7.
[12] Kanoglu M, Bolatturk A, Yilmaz C. Thermodynamic analysis of models used in hydrogen production by geothermal energy. Int J Hydrogen Energy 2010;35:8783–91.
[13] Yilmaz C. Optimum energy evaluation and life cycle cost assessment of a hydrogen liquefaction system assisted by geothermal energy. Int J Hydrogen Energy 2020;45:3558–68.
[14] Yilmaz C, Kanoglu M, Bolatturk A, Gadalla M. Economics of hydrogen production and liquefaction by geothermal energy. Int J Hydrogen Energy 2012;37:2058–69.
[15] Yilmaz C, Kanoglu M, Abusoglu A. Exergetic cost evaluation of hydrogen production powered by combined flash-binary geothermal power plant. Int J Hydrogen Energy 2015;40:14021–30.
[16] Bouchareb-Haouchine FZ, Boudoukha A, et Haouchine A. Hydrogéochimie et geothermometrie: apports à l'identification du réservoir thermal des sources de Hammam Righa, Algérie. Hydrol Sci J 2012;57(6):1184–95.
[17] Holdmann G, List K. The Chena Hot Springs 400 kW geothermal power plant: experience gained during the first year of operation. Trans Geoth Resour Counc 2007;31:515–9.
[18] Ganjehsarabi H. Mixed refrigerant as working fluid in Organic Rankine Cycle for hydrogen production driven by geothermal energy. Int J Hydrogen Energy 2019;44:18703–11.
[19] Chávez-Urbiola EA, Vorobiev YV, Bulat LP. Solar hybrid systems with thermoelectric generators. Sol Energy 2012;86:369–78.
[20] Zare V, Palideh V. Employing thermoelectric generator for power generation enhancement in a Kalina cycle driven by low-grade geothermal energy. Appl Therm Eng 2018;130:418–28.
[21] Khanmohammadi S, Saadat-Targhi M, Ahmed FW, Afrand M. Potential of thermoelectric waste heat recovery in a combined geothermal, fuel cell and organic Rankine flash cycle (thermodynamic and economic evaluation). Int J Hydrogen Energy 2020;45(11):6934–48.
[22] Ziapour BM, Saadat M, Palideh V, Afzal S. Power generation enhancement in a salinity-gradient solar pond power plant using thermoelectric generator. Energy Convers Manag 2017;136:283–93.
[23] Gholamian E, Habibollahzade A, Zare V. Development and multi-objective optimization of geothermal-based organic Rankine cycle integrated with thermoelectric generator and proton exchange membrane electrolyzer for power and hydrogen production. Energy Convers Manag 2018;174:112–25.
[24] Ghazvini M, Sadeghzadeh M, Ahmadi MH, Moosavi S, Pourfayaz F. Geothermal energy use in hydrogen production: a review. Int J Energy Res 2019;43:7823–51.
[25] Merienne R, Lynn J, McSweeney E, O'Shaughnessy SM. Thermal cycling of thermoelectric generators: the effect of heating rate. Appl Energy 2019;237:671–81.
[26] Omer G, Yavuz AH, Ahiska R, Calisal KE. Smart thermoelectric waste heat generator: design, simulation and cost analysis. Sustain Energy Technol Assessments 2020;37:100623.
[27] Thermoelectric module reliability. Thermoelectric n.d. https://thermal.ferrotec.com/technology/thermoelectric-reference-guide/thermalref10/. [Accessed 28 August 2020].
[28] London AL, Seban RA. A generalisation of the methods of heat exchanger analysis. Int J Heat Mass Tran 1980;37:5–16.
[29] Ulleberg Ø, Mørner SO. TRNSYS simulation models for solar-hydrogen systems. Sol Energy 1997;59:271–9. https://doi.org/10.1016/S0038-092X(97)00015-7.
[30] Mraoui A, Menia S. Renewable electrolytic hydrogen potential in Algeria. Int J Hydrogen Energy 2019;44:26863–73. https://doi.org/10.1016/j.ijhydene.2019.08.134.
[31] JRC photovoltaic geographical information system (PVGIS) - European commission n.d. https://re.jrc.ec.europa.eu/pvg_tools/en/tools.html#TMY. [Accessed 17 May 2020].

[32] Hsu C-T, Huang G-Y, Chu H-S, Yu B, Yao D-J. Experiments and simulations on low-temperature waste heat harvesting system by thermoelectric power generators. Appl Energy 2011;88:1291–7. https://doi.org/10.1016/j.apenergy.2010.10.005.
[33] Ahiska R, Mamur H. Design and implementation of a new portable thermoelectric generator for low geothermal temperatures. IET Renew Power Gener 2013;7:700–6. https://doi.org/10.1049/iet-rpg.2012.0320.
[34] Ahiska R, Mamur H. Development and application of a new power analysis system for testing of geothermal thermoelectric generators. Int J Green Energy 2016;13:672–81. https://doi.org/10.1080/15435075.2015.1017102.
[35] Liu C, Chen P, Li K. A 1 KW thermoelectric generator for low-temperature geothermal resources. Stanford, California, USA: 39th Workshop on Geothermal Reservoir Engineering; 2014. p. 24–6.
[36] Liu C, Chen P, Li KA. 500 W low-temperature thermoelectric generator: design and experimental study. Int J Hydrogen Energy 2014;39:15497–505. https://doi.org/10.1016/j.ijhydene.2014.07.163.
[37] Gibson TL, Kelly NA. Predicting efficiency of solar powered hydrogen generation using photovoltaic-electrolysis devices. Int J Hydrogen Energy 2010;35:900–11.
[38] Gibson TL, Kelly NA. Optimization of solar powered hydrogen production using photovoltaic electrolysis devices. Int J Hydrogen Energy 2008;33:5931–40. https://doi.org/10.1016/j.ijhydene.2008.05.106.